IEEE Access
Multidisciplinary ⋮ Rapid Review ⋮ Open Access Journal

Received 16 October 2022, accepted 15 November 2022, date of publication 17 November 2022,
date of current version 30 November 2022.

Digital Object Identifier 10.1109/ACCESS.2022.3223051

RESEARCH ARTICLE

Reliability Analysis on Winding Configurations of Variable Reluctance Resolver Under Faulty Conditions

MAHDI EMADALESLAMI[1], (Student Member, IEEE), MOHAMMADSADEGH KHAJUEEZADEH[2], MOHAMMADEBRAHIM ZAREI[1], MAHMOUDREZA HAGHIFAM[1], (Senior Member, IEEE), AND HADI TARZAMNI[3], (Student Member, IEEE)

[1]Department of Electrical and Computer Engineering, Tarbiat Modares University, Tehran 14117-13116, Iran
[2]Electrical Engineering Department, Sharif University of Technology, Tehran 11365-8639, Iran
[3]Department of Electrical Engineering and Automation, Aalto University, 02150 Espoo, Finland

Corresponding author: Hadi Tarzamni (hadi.tarzamni@aalto.fi)

This work was supported by the Finnish Electronic Library (FinElib), Finland, under the FinELib Consortium's Agreement with IEEE.

ABSTRACT Owing to the use of the Permanent Magnet Synchronous Motor (PMSM) widely in Electrical Vehicles (EVs), the mandatory existence of rotor angle sensor in its control algorithm, higher reliability of the resolver than the other instance, and eventually, the significant effect of resolver errors on the system stability, comparing the reliability of two winding configurations in resolver is regarded analytically and numerically in the following study. Firstly, the employed assessment model is defined. Subsequently, it is necessary to investigate the failure modes in the resolver thoroughly. Among the methods used to assess reliability, the Markov model is chosen for the reliability analysis. Finally, by using an experimentally verified Finite Element (FE) resolver model, the faulty conditions in the Variable Turn Overlapping Winding (VTOW) and Constant Turn Non-Overlapping Winding (CTNOW) configurations of the Variable Reluctance (VR) resolver are investigated. The accuracy degradation of the resolver under faulty conditions is used as the reliability criteria to define the reliability state of the resolver.

INDEX TERMS Variable reluctance (VR) resolver, constant turn non-overlapping winding (CTNOW), variable turn overlapping winding (VTOW), finite element analysis (FEA), reliability analysis, Markov model.

I. INTRODUCTION

Priority choice in Electric Vehicles (EVs) according to constraints such as efficiency, power density, and availability with considering size simultaneously will be Permanent Magnet Machines (PMMs). During the usage of PMMs, owing to the sensitivity of the uses and the imposing costs in the following of PMMs' and drives' error, some concerns such as fault tolerability, operating continuously, and capacity to withstand environment variations and conditions has high priority. Accordingly, some investigations have recently regard-ed the reliability study of PMM and its drive systems. In [1], the effect of various design configurations of the Flux Switching Permanent Magnet (FSPM) machine, particularly the stator core topology, hybrid excitation, and winding arrangement, on reliability has been investigated. The effect of faults in drive and motor constructions reliability such as switches, windings, and PM has been investigated through the Markov model. In [2], a methodology for reliability assessment of an in-duction motor drive systems with Field Oriented Control (FOC) algorithm, including the electric machine, electronics circuit, and sensors, has been given through the Markov reliability modeling. As the control algorithm of PMMs, especially FOC, has a extreme dependency on sensor for detecting rotor angle, the reliability of the employed sensor must be thoroughly investigated in

The associate editor coordinating the review of this manuscript and approving it for publication was Lorenzo Ciani.

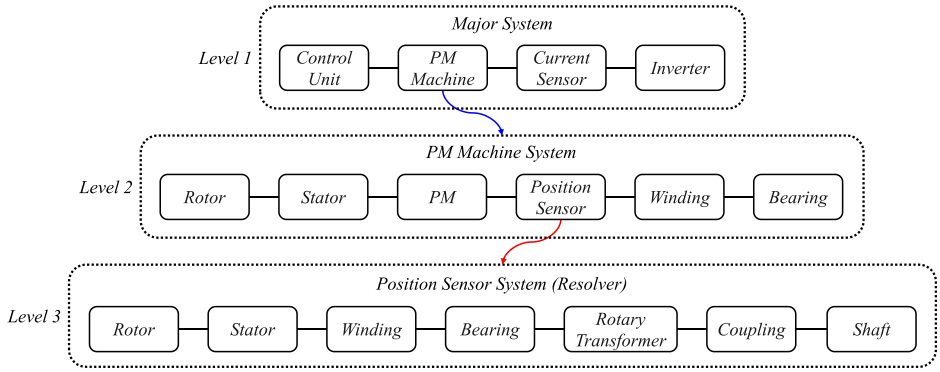

FIGURE 1. Reliability block diagram of the PMM drive system.

PMMs drive with the FOC algorithm. However, [1] and [2] have only regarded omission and damage modes of the rotor angle sensor and neglected its configuration physically and practically during the reliability study of the drive set.

Among the widely used sensors for detecting rotor angle in the inverter-driven motors, such as encoder, Hall effect element, and resolver, the latter is more satisfactory owing to higher tolerability in harsh environments. On the other hand, the accuracy of the resolver in various conditions must be consistent and steady. Thus, it is necessary to investigate the resolver's reliability in faulty conditions resulting from dust, moisture, warmth, vibrations, noise, and stresses.

As the PMMs drive stability is highly sensitive to the accuracy of the resolver, various resolver configurations have been investigated and suggested to have better accuracy and higher reliability. In a reliability study, optimizing the configurations to achieve more tolerability in faulty conditions is valuable. Hence, in [3] and [4], more accuracy and lower degradation under Short Circuit (SC) and eccentricity have yielded by modifying the winding arrangement and adding damping to the rotor winding of the Wound Rotor (WR) resolver. Moreover, [5] and [6] have optimally designed a rotor contour of a Variable Reluctance (VR) resolver to achieve higher accuracy and tolerability under faulty conditions. During the investigations on the resolver, its reliability has been regarded descriptively. Accordingly, the VR and WR resolver configurations have frequently been investigated against each other in the reliability concern. Repeatedly said, the VR resolver has more reliability than the WR owing to the non-wound rotor, and the no need to slip rings, brushes or Rotary Transformer (RT) [6], [7], [8]. On the contrary, VR is more sensitive to eccentricity than WR [8]. Also, the WR and the VR will be extremely sensitive to SC in signal and excitation winding [8].

Similarly, the confrontation between the two winding configurations of VR resolver, including Variable Turn Overlapping Winding (VTOW) and Constant Turn Non-Overlapping Winding (CTNOW), have been regarded previously by others. Owing to the simplicity and cost of manufacturing, the constant number of winding turns, and the non-overlapping configuration of the resolver's winding, CTNOW is widely chosen. However, either VTOW or CTNOW configurations are sensitive to SC fault and eccentricity [9]. On the other hand, the accuracy of the resolver when using the VTOW is significantly higher. Though, the design and use of a resolver regarding the environment and operating conditions will have such complexity and sensitivity, its reliability has not been investigated analytically and quantitatively, to the best of the author's knowledge. So, this has led the authors to do a study from the reliability view to choose which of the above winding configurations gives better reliability under analogous conditions, regardless of manufacturing cost and complexity.

The following study gives a thorough scheme of the resolvers' reliability analysis by the Markov model. Accordingly, after specifying a satisfactory assessment model, system failure modes, reliability criteria, and assessment method, the reliability of two winding configurations, including VTOW and CTNOW, in the VR resolver is analyzed comprehensively under various faulty conditions. Consequently, the better configuration in term of reliability is chosen based on Markov's analysis. Finally, to ensure the accuracy of the used FEA, a prototype of investigated 1-X VR resolver with CTNOW configuration was built and tested experimentally.

II. RELIABILITY ASSESSMENT PROCEDURE

Prior to any reliability assessment, it is necessary to specify a satisfactory assessment model, failure modes, reliability criteria, and an assessment method.

A. ASSESSMENT MODEL

A PMM drive system consists of control drive unit, inverter circuit, electric machine, current sensor, and rotor angle sensor. Since any fault occurrence in the sub-systems can degrade the operating of the drive system, the reliability modeling at the drive stage can be shown as Level 1 in Fig. 1. In [1], [2], [10], and [11], drive stage reliability is investigated, thoroughly. According to the energy conversion duty, the PM motor is more subjected to electrical and mechanical stresses than the other sub-systems. So, it must be given more concern.

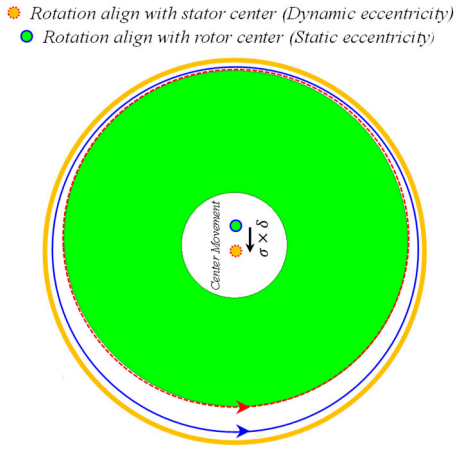

FIGURE 2. Overview of rotor and stator movement and rotation path in resolver eccentricity condition.

Drive existence is mandatory because the magnetic field and variable frequency source are necessary for PM motors. Thus, the resolver is necessary to detect rotor angle during the motor control drive.

Depending on the design and configuration, the resolver consists of windings, rotor, stator, brushes, RT, shaft, coupling, cage, and bearings. The resolver is a so-called synchronous generator with two sine and cosine signal windings, which rotates synchronously with the primary motor. Rotation of the rotor induces voltage signals, which have a 90-degree shifting in windings configuration. The excitation windings is fed by a high-frequency voltage source. The processing of sine and cosine signals of the resolver is necessary for extraction of rotor angle, which the Resolver to Digital Converter (RDC) handles [12], [13]. Since any fault in the resolver's sub-systems will cause the resolver's failure, the reliability modeling of a WR resolver is shown as Level 3 in Fig. 1, considering the excitation is fed through an RT. Any variation in the resolver configuration might cause a change in the block diagram modelling, but the reliability analysis remains unchanged and analogous among all configurations. Accordingly, for the WR configuration displayed as Level 3 in Fig. 1, the reliability ($R_{WR}(t)$) and Mean Time to Failure (MTTF) will be written as follows [14]:

$$R_{WR}(t) = \prod_{i=1}^{N} R_i = e^{-\sum_{i=1}^{N} \lambda_i t} \tag{1}$$

$$MTTF = \int_0^{\infty} R(t)\, dt \tag{2}$$

where R and λ are the reliability and failure rate, respectively, and N is the number of failure modes. Details about λ is given in section II. E.

B. FAILURE MODE

Occurring faults in each sub-system of the resolver, including windings, rotor, stator, brushes, RT, shaft, coupling, and bearings, affect the resolver's reliability and availability. Thus, the resolver's reliability would be investigated by identifying and evaluating the failure modes and their corresponding states' probability.

Owing to the similarity between resolvers and electric machines, structurally and operationally, it is necessary to recognize the dissimilarity of the faults' cause and manner [8], [15]. Contrary to the motor, the resolver shaft does not carry any external load, so excessive overload would not occur. Moreover, following the connection of the resolver windings to the RDC and the negligible current of signal windings, faulty conditions, such as winding overheating and insulating breakdown, do not occur. While, the insulation injury occurs with careless winding.

1) ECCENTRICITY

Even in newly made resolvers, wrong manufacturing or mounting might lead to static eccentricity. During the static eccentricity, the stator axis does not coincide with the rotor and rotation axes, in which the location of minimum and maximum airgap length is constant. Subsequently, it will inject error in rotor angle estimation, followed by vibrations in the primary motor. Another type of eccentricity occurs dynamically, so-called dynamic eccentricity, when the rotor axis does not coincide with the axis of rotation and the stator one, in which the location of the minimum/maximum airgap length is not constant while its length is constant. Accordingly, mixed eccentricity occurs when none of the stator and rotor axes coincide with the rotation axis, and both the location and length of the minimum/maximum airgap length have a dependency on time. By considering σ as the eccentricity index, $\sigma \times \delta$ is the eccentricity intensity. The stator and rotor rotation during static and dynamic eccentricity, respectively, is shown in Fig. 2 [16]. Accordingly, where $\sigma = 0$ resolver is in healthy condition.

2) RUNOUT

Axial backlash and imposing it on the resolver, especially in motors with a vertical drive, causes a change in the airgap length in axial flux resolver and the coupling value between the rotor and stator in radial flux resolver so that the runout will occur [7].

3) OPEN CIRCUIT

Since the current of the signal windings is negligible, wires are extremely thin. So, the possibility of faults such as SC and Open Circuits (OC) in the resolver under heat, vibration, and wrong mounting will be significantly high. When an OC occurs in the excitation winding, the resolver is entirely out of service. Additionally, if OC occurs in either signal windings, the rotor angle is lost [17].

4) SHORT CIRCUIT

During SC, the damage severity can sometimes be minor and not disable resolver functionality. Two types of SC are regarded in the resolver, Turn-to-Turn SC (TTSC), in which a short circuit occurs between the turns of one winding, and Phase-to-Phase SC (PPSC), in which the short circuit occurs

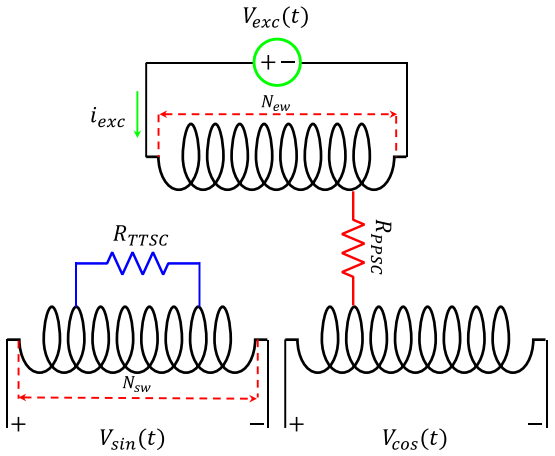

FIGURE 3. Windings diagram in healthy and faulty condition with inter-turn and Phase-to-Phase SC fault.

between turns of two or more adjacent windings. A PPSC is more likely to occur when windings have an overlapping configuration. By considering R_{TTSC}, R_{PPSC}, N_{sw}, and N_{ew} as the TTSC fault resistance, the PPSC fault resistance, total number of signal winding turns, and total number of excitation winding turns, respectively, when $R_{TTSC}, R_{PPSC} \rightarrow \infty$ resolver windings are in healthy condition. On the contrary, when $R_{TTSC}, R_{PPSC} = 0$, the highest intensity of SC fault occurs. The SC fault modeling is shown in Fig. 3 [9].

5) ROTARY TRANSFORMER

The excitation winding is fed through brushes or RT in the WR resolver, which excitation windings are on the rotor. A dirty and warm ambient and even wrong maintenance will intensify the possibility of wearing brushes and interrupting the excitation supply. The faults on the RT, such as the resolver, are categorized as eccentricity, SC, and OC.

Using the resolver along with a cage will bring bearings, a shaft, and a coupling to the resolver system, where each above suffers from some faults. Accordingly, the vibrations, regardless of origin in the resolver or the primary motor, will cause failures such as wear and fatigue of the flexible coupling and the bearings [18], [19].

C. EVALUATION CRITERIA

Since resolver accuracy degradation significantly affect the motor drive system stability, the resolvers' faulty conditions must be investigated based on the drive system and satisfactory reliability criteria. Accordingly, by exceeding the criteria values from allowable limits, under faulty conditions, the system's state is signified as fail by "F", and if it continues within the allowable limits, the system state will remain reliable, denoting by "R". Accordingly, the main criterion for evaluating the resolvers' accuracy is the Average of Absolute Position Error (AAPE). The AAPE limit value will be 0.5 degrees based on no-derating in control system stability.

TABLE 1. Parameters of bearing's failure rate calculation.

Symbol	Value	Symbol	Value
L_S	438.377 (lb)	Y	0.87
L_A	$X.FR + Y.FA =$ 1.075 (lb)	FR	0.503 (lb)
X	0.41	FA	0.998 (lb)
$C_t, C_{R,} C_{SF}$	1	C_V	0.645
C_{CW}	2.234	C_C	1.8
y	3	n	1500 (rpm)

D. EVALUATION METHODS

In the motor reliability assessment Markov method is more satisfactory since the system's behavior changes with time. In the Markov modeling, the system's next state have a dependency on the current state. The above theory means the constant value of λ, as in electrical systems. Another advantage of the Markov model is the consideration of faulty condition alongside healthy and fail conditions. Accordingly, Markov modeling has been used in our study to assess the resolver's reliability. One of the most common ways to obtain the Markov modeling is to use the Chapman–Kolmogorov, which is shown below [20]:

$$P'(t)^T = A^T.P(t)^T \tag{3}$$

where $P(t)$ and A are state probability matrix and transition probability between the Markov chains, respectively. If the Markov model has n states, the [P] matrix will be written as (4), which shows the probability of being in the i^{th} state at the t^{th} time.

$$P(t) = \left[P_1(t)\ P_2(t)\ \ldots\ P_n(t) \right] \tag{4}$$

Accordingly, A will be written as (5), shown at the bottom of the next page, the sign will be "+" and "-" among transferring in and out of states, respectively. Namely, λ_{1n} means the failure rate from state 1 to state n and μ_{n1} means the maintenance rate from state n to state 1. By solving (3), the probability of being in any of the states of the Markov chain will be shown. So, summing the probability of being in reliable states gives the system reliability.

E. FAILURE RATE

The basis of a system reliability analysis is the failure rate. Accordingly, The Bathtub curve shows the overview of a lifetime, including the infant mortality stage, the useful life, and the wear-out stage, respectively. The useful life is the best operating time where the failure rate is constant and low, and the operating cost is lower than the wear-out stage, where repairing is vital periodically. Commonly, when operating conditions are in useful life, two methods are noteworthy for predicting failure rates; the Parts Count Analysis (PCA) and the Part Stress Analysis (PSA). The above methods differ in the degree of statistical data. Although, the PCA causes a more conservative failure rate estimation [21]. While [22] and [23] are the most valid guide for calculating failure rate, the

failure rate is written as follows:

$$\lambda = \lambda_{base} \times \prod_i \pi_i \times \alpha \times \pi_{induced} \times AF \tag{6}$$

where, λ_{base} is the basic failure rate and manufacturer generally gives it, π_i is the stress factor, and α is the probability that each failure modes will occur. $\pi_{induced}$ and Acceleration Factor (AF) show the cage effect [24].

In the resolver, the cage (frame) is used to mitigate mechanical risk, Electromagnetic Interference (EMI), and magnetic interference, especially owing to the existence of magnetic brake and leakage flux (magnetic stray) in PMSMs. In this regard, $\pi_{induced}$ shows the effect of EMI. Additionally, cage usage has significant effects on the resolver installation, which adds bearings, shafts, and coupling. Accordingly, the resolver's mounting is no longer done directly on the rotor shaft like the frameless structure. So, the resolver's vibration severity originated by the motor due to the damping increase will be significantly changed. Moreover, cage usage also mitigates the effects of dust and moisture. Thus, the effect of vibration and environment on the resolver failure rate can be shown by using AF [24], [25].

It is mandatory to thoroughly recognize the resolver's construction to obtain the resolver failure rates. Accordingly, the resolver does not take any external loads, and only two types of radial and axial loads are on the bearing due to its physical structure. On the other hand, the probability of misalignment and bent shaft in the resolver and motor sets is significant. Consequently, the ball bearing is chosen for increasing resolver reliability [26], [27], [28], owing to its lower contact surface and load bearing, ball-shaped design, and higher tolerability than other bearing types. the ball bearing failure rate, according to [23] and (6), is written as (7)-(9). So, the coefficients data is given in Table 1 for calculating the stress. Besides ball bearing, the flexible coupling mitigates shock and load effects in drive systems, which have vibrations.

$$\begin{aligned}\lambda_{BE} &= \lambda_{BE,B} \cdot C_R \cdot C_V \cdot C_{CW} \cdot C_t \cdot C_{SF} \cdot C_C \\ &= 3.5 * 10^{-9}/h \end{aligned} \tag{7}$$

$$\lambda_{BE,B} = \frac{1}{L_{90h}} = 0.001327 * 10^{-6} \tag{8}$$

$$L_{10h} = \frac{10^6}{60n}\left(\frac{L_S}{L_A}\right)^y = 753.54 * 10^6 \tag{9}$$

Additionally, calculating resolver windings' failure rates will be written by considering the probability of failure modes and employing the standards. Accordingly, the resolver failure rate in the MIL-HDBK-217F [21] while the ambient heat is

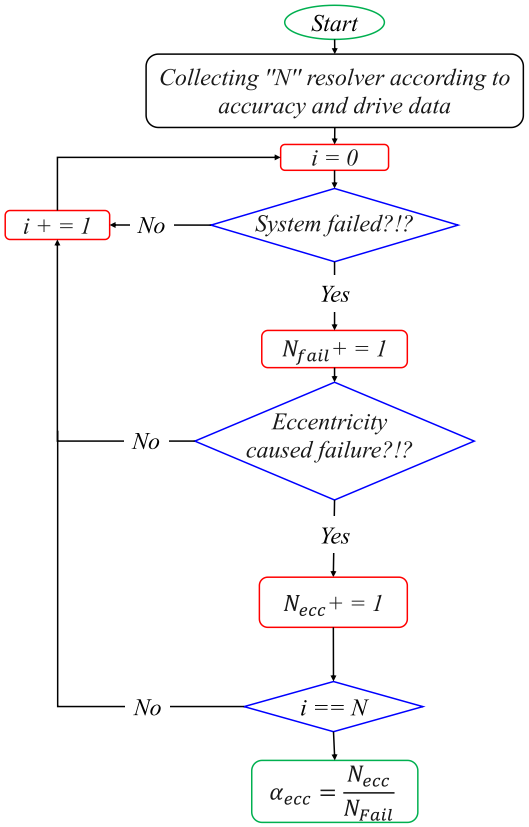

FIGURE 4. Guide to calculating the eccentricity failure rate in resolvers.

30°C and the resolver is employed on the vehicle will be as follow:

$$\lambda = \lambda_{base} * \pi_S * \pi_E \tag{10}$$

$$\lambda_{base} = 0.00535 * e^{\left(\frac{T_F+273}{334}\right)^{8.5}} \tag{11}$$

$$T_F = 40°\text{C} + Ambient\ Temperature \tag{12}$$

In (10), π_S and π_E are the size factor and the environment factor, respectively. Also T_F shows the frame heat. Accordingly, λ_{base} is $680{*}10^{-9} Failure/h$. On the other hand, in FDM-91, the percentage of resolver's winding failure is 45% and $\lambda_{winding}$ is $306 * 10^{-9} Failure/h$. Moreover, the percentages of winding faults category including OC, SC, and Phase to Phase SC (PPSC) are 42%, 42%, and 16%, respectively.

Among resolver faults, eccentricity is caused by stator and rotor movement and can cause the system to fail under reliability criteria. Although it emerges in the system by stator and rotor movement, it will lead to the drive system failure

$$A = \begin{bmatrix} -\sum_{i=1}^{n} \lambda_{1i} & \mu_{11} & \cdots & \mu_{(n-1)1} & \mu_{n1} \\ \lambda_{12} & -(\sum_{i=1}^{n} \lambda_{1i} + \mu_{11}) & \cdots & \mu_{(n-1)2} & \mu_{n2} \\ \cdots & \cdots & \ddots & \cdots & \cdots \\ \lambda_{1(n-1)} & \lambda_{2(n-1)} & \cdots & -(\lambda_{(n-1)n} + \sum_{i=1}^{n-2} \mu_{(n-1)i}) & \mu_{n(n-1)} \\ \lambda_{1n} & \lambda_{2n} & \cdots & \lambda_{(n-1)n} & -\sum_{i=1}^{n-1} \mu_{ni} \end{bmatrix} \tag{5}$$

TABLE 2. Failure rate of resolver's faulty conditions.

Failure modes	Value *	Failure modes	Value *
Static Eccentricity	249.34	Open Circuit	128.52
Dynamic Eccentricity	124.67	Brush	3200
Excitation SC	128.52	Bearing	3.5
Signal SC	128.52	Phase to Phase SC	48.96
Rotary Transformer	86.4		

* $(10^{-9}Failure/h)$

TABLE 3. Main failure modes of resolvers according to location and cause.

Fault Location	Failure Mode	Failure Cause
Rotor	Dynamic Eccentricity Run out	Vibration Axial backlash
Stator	Static Eccentricity	Manufacturing erroneous Awkward mounting Motor bearings damage Motor gearbox damage
Winding	Short Circuit (Turn to Turn) Short Circuit (Phase to Phase) Open Circuit	Scratch of insulation High ambient warmth Vibration Mechanical shock
Brush	Worn brush Brushes fail opening	High ambient warmth Contamination Wrong maintenance
RT	Eccentricity Short Circuit	Same as resolver sources
Shaft	Shaft Misalignment	Wrong assembly
Bearing	Fatigue Damage Bearing Vibration	Excessive vibration Misalignment
Coupling	Fatigue or flexing element Worn flexing element	Torsional Vibration Excessive shaft misalignment

before it leads to stator and rotor failure. Accordingly, the effect of eccentricity is seen sooner in the drive system rather than in the stator and rotor physical construction. The calculating methodology of the dynamic and static eccentricity failure rates is displayed in Fig. 4. By considering the fault diagnosis algorithms, we can first diagnose the faults based on resolver signals, motor operating, and reliability criteria. The suggested method to obtain the eccentricity failure rate can be useful for resolver manufacturers. In the following study, owing to constraints and lack of access to accurate data, the failure rate of this fault is shown approximately in Table 2 and used in section III. According to [1], fortunately, the failure rate values are only used numerically to assess, and failure rate values will not affect the reliability assessment methodology.

Any error in the resolver causes degradation in the control drive stability of the PMS motor. As shown in Table 3, one of the main sources of fault in the resolver is the existence of vibrations in the drive set and its transmitting to the resolver [29], [30]. Consequently, faults such as eccentricity and SCs in the resolver, if not fixed, gradually intensify to the degree that leads to system failure. While other faults such as bearing, shaft, coupling, OC, and PPSC immediately cause the system failure. Thus, our study investigates the effect of eccentricity and SCs by increasing the fault intensity and other faults on the resolver reliability based on the assessment criteria.

III. RELIABILITY ANALYSIS OF WINDING CONFIGURATIONS IN VARIABLE RELUCTANCE RESOLVER

The two winding configurations, VTOW and CTNOW in VR resolver, as shown in Fig. 5, have been investigated. The CTNOW configuration is widely chosen in VR resolvers, owing to the winding simplicity, cost-effectiveness, constant turns number, and non-overlapping configuration. On the other hand, both VTOW and CTNOW have a significant vulnerability to SC fault and eccentricity. Although, the accuracy of the resolver in using the VTOW is higher. So, in the following, it will be shown which winding configurations (VTOW or CTNOW) give better reliability in the VR resolver's faulty

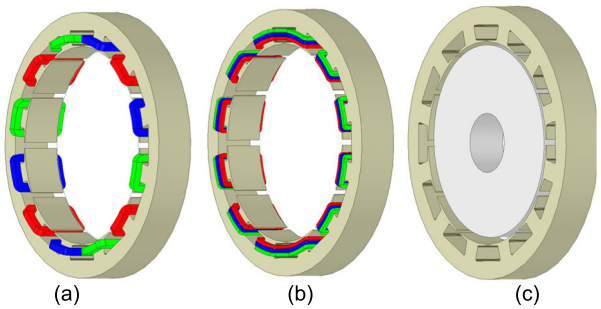

FIGURE 5. Schematic of the analysed VR-resolver. (a) Constant Turn Non-Overlapping Winding (CTNOW). (b) Variable Turn Overlapping Winding (VTOW). (c) 12-tooth stator and 1-X rotor contour.

conditions, regardless of manufacturing cost and complexity. This study investigates a 1-X VR resolver with a 12-teeth stator, $G_{max} = 2mm$, and $G_{min} = 0.5mm$ for the above two winding configurations [5]. This reliability analysis can be a guide to choose the VR resolver winding configuration optimally.

First, the corresponding Markov model must be derived to study the effect of the winding configuration on the resolver's reliability. Hence, applying all common faulty conditions to the resolver with each winding configuration is necessary to identify the system state under reliability criteria. By Taking signal SC fault of 2 turns, as a case, Fig. 6 show the accuracy degradation of the resolver with VTOW and CTNOW configurations. Table 4 shows that VTOW and CTNOW under signal SC faults of 2 turns are R and F states, respectively. As said before, the reliability state is based on assessment criteria, which in our study is AAPE = 0.5 Deg. So, AAPE = 0.703 Deg is more than our criteria, and its state will be known

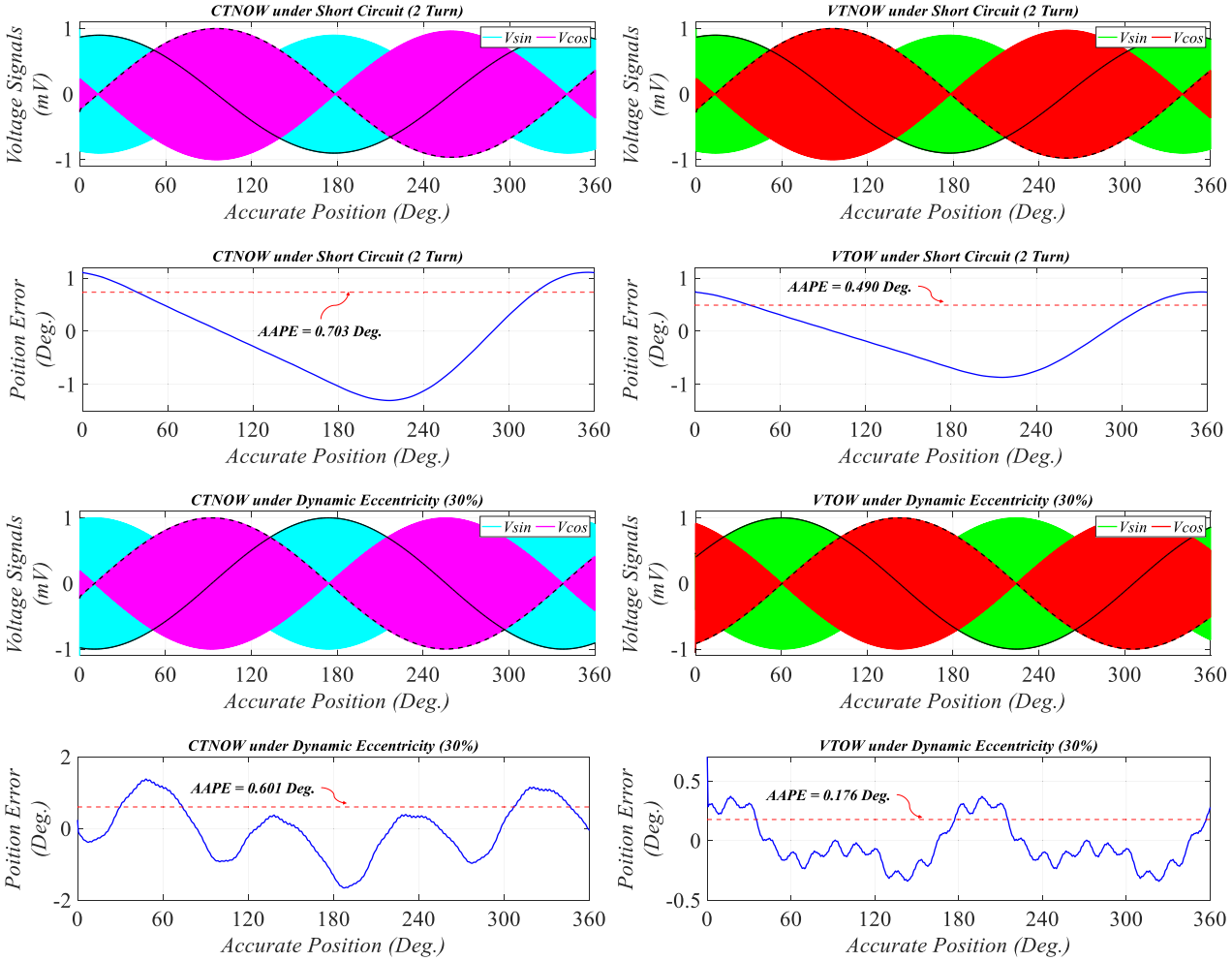

FIGURE 6. Position errors and voltage signals (Normalized) of two winding configuration of 1-X VR resolver under signal winding 2 Turns (2T) short circuit and dynamic eccentricity.

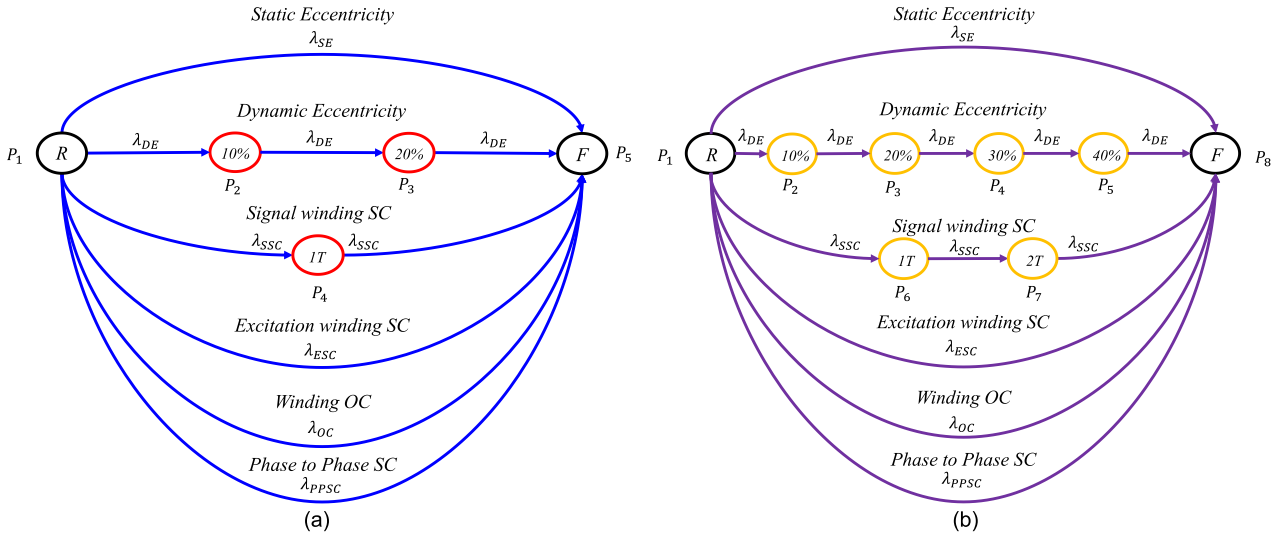

FIGURE 7. Markov models under reliability analysis. (a) CTNOW. (b) VTOW.

as the F state in the CTNOW configuration. Similarly, for AAPE = 0.490 Deg, the R state is known.

According to the above, all faulty conditions are injected into the resolver system. Outcomes of Finite Element

TABLE 4. Reliability status of two winding configurations under the main faults.

Type of Winding	Type of Fault	Intensity	AAPE (Deg.)	Status
CTNOW	Healthy	-	0.038	R
	Static Eccentricity	10%	0.696	F
	Dynamic Eccentricity	10%	0.065	R
		20%	0.233	R
		30%	0.601	F
	Signal SC	1T	0.339	R
		2T	0.703	F
	Excitation SC	1T	8.623	F
VTOW	Healthy	-	0.004	R
	Static Eccentricity	10%	0.662	F
	Dynamic Eccentricity	10%	0.007	R
		20%	0.011	R
		30%	0.176	R
		40%	0.352	R
		50%	0.528	F
	Signal SC	1T	0.245	R
		2T	0.490	R
		3T	0.736	F
	Excitation SC	1T	21.486	F

Analysis (FEA) are given in Table 4 and Fig. 7. Table 4 shows the Markov modeling states of the VTOW and CTNOW configuration in Fig. 7(a)-(b). Accordingly, in Fig. 8(a) for VTOW configuration, P1 shows the R state for each scenario with no fault, P2 to P5 define the R states of dynamic eccentricity under %10 to %40 with a severity size of 10%, P6, P7 define the R states of signal winding SC fault under 1 and 2 turns respectively, and P8 defines the F state. According to (5), [A] matrix size for VTOW and CTNOW is 8×8 and 5×5, respectively.

By substituting [A] into (4), the probability of each state can be obtained and shown in Fig. 8. According to Fig. 8(a), starting from state one (R state), while decreasing the probability of being in the R state, the probability of being in other states (P2-P7) grows, called Transient States (TS), and then goes to a constant value, called Steady State (SS). Finally, after a long time (30 years), the system converges to the absorbing state (P8) and stays in it. By substituting the probability of each state into (1), the reliability of VTOW, $R_{VTOW}(t)$ and CTNOW, $R_{CTNOW}(t)$ can be written as (13) and (14), respectively.

According to [9], and the Markov analysis in Fig. 8 confirm, the VTOW configuration has more reliability under the signal SC fault, dynamic eccentricity fault, and overall operating. Also, it has more tolerability in high fault degrees of severity, owing to that the windings in the VTOW have more sinusoidally distributing than in the CTNOW configuration, resulting in more mitigation and (13)–(18), as shown at the bottom of the next page, attenuation of faults effect, as can be seen in Fig. 9. Accordingly, the reliability metric of the investigated winding configurations in SC and dynamic eccentricity fault scenarios are as (15)-(18).

Finally, using (13) and (14), the MTTF of VTOW and CTNOW configurations are 19.77 and 11.3 years,

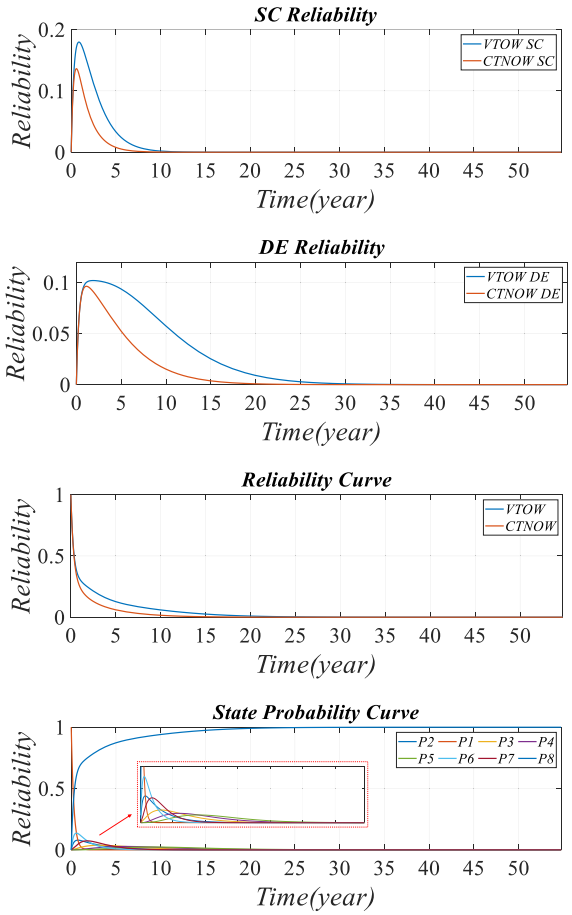

FIGURE 8. Curves of reliability analysis for CTNOW and VTOW configurations.

respectively. Based on the MTTF analysis, we can hope that any resolver with a VTOW configuration works for an average of 19.77 years before it fails.

IV. EXPERIMENTAL VERIFICATION OF THE FINITE ELEMENT RESOLVER MODEL

In the above reliability study of VR resolvers with VTOW and CTNOW configurations, a 2D time-stepping FE modeling was the main tool to analyse and investigate the resolver's faulty conditions, which its mesh quality and flux density is shown in Fig. 10. Accordingly, the accuracy of the TS-FEM must be verified experimentally. So, the investigated 1-X VR resolver with a 12-teeth stator is built and practically tested. The stator and the rotor of the built resolver are shown in Fig. 11. The prototype resolver is tested using the test circuit in Fig. 12. Fig. 12 shows the coupling of the VR resolver to a dual-shaft DC motor with adjustable angular velocity. As the ideal sensor, a programmable encoder is used to detect the rotor angle of the DC motor. Supplying the excitation windings is by a digitally synthesized function generator. The excitation voltage magnitude is adjusted by an automatic gain control circuit of the function generator. The excitation frequency is set to 5 kHz with a sampling frequency of 0.1 Hz. The excitation voltage is shown using

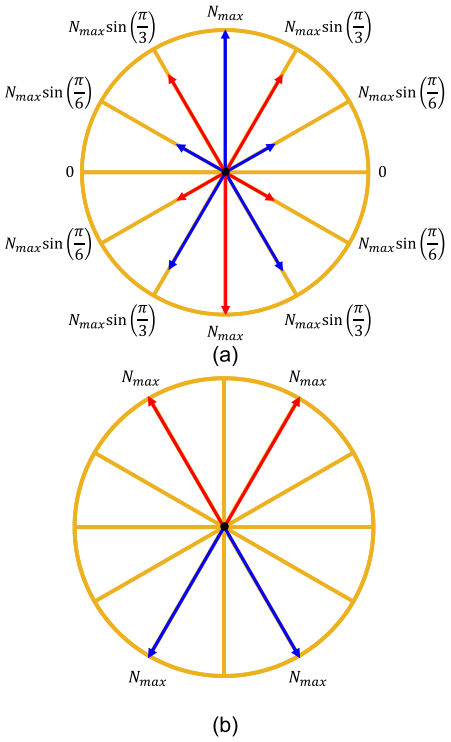

FIGURE 9. Distributing of signal winding in two conventional configurations. (a) Variable Turn Overlapping Winding (VTOW). (b) Constant Turn Non-Overlapping Winding (CTNOW).

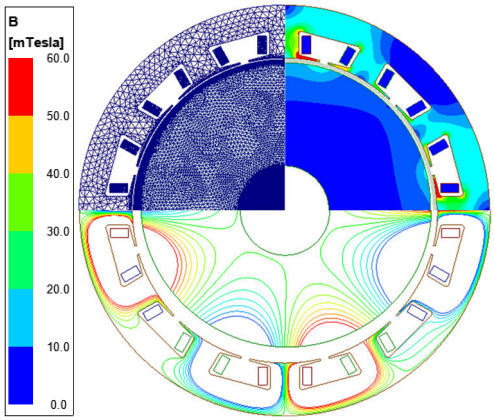

FIGURE 10. Schematic of the mesh grid, magnetic flux density, and magnetic flux lines on the studied 1-X VR resolver with CTNOW configuration.

FIGURE 11. Prototype 1-X VR resolver with CTNOW configuration. (a) Stator and (b) Rotor.

an analog oscilloscope in Fig. 12. Finally, the signal voltages are saved using a digital oscilloscope, as shown in Fig. 12. The MATLAB software is used for processing the signal voltages to avoid the compensating effect of RDC through the Peak Detection Method (PDM). Comparing the resolver rotor angle with the encoder leads to calculating the resolver accuracy degradation as an error. The value of AAPE and the Maximum Position Error (MPE) as the best metrics for evaluating the resolvers' accuracy are shown for FEM and the prototype model in Fig. 13. It can be seen the AAPE and the MPE are 0.042° and 0.068° for built resolver, respectively. Moreover, AAPE and the MPE are 0.038° and 0.064° for FEM, respectively. In the worst case, the error between the FEM and prototype is less than 10%. For the sake of saving time, the test was only in CTNOW configuration, which has lower accuracy. Accordingly, the FEM resolver model is verified experimentally.

Implementing faulty conditions in the resolver is hard experimentally or leads to resolver damage entirely, including dynamic eccentricity, OC, and SC. Accordingly, static eccentricity was injected into the resolver system by manufacturing a damaged stator frame. The investigation of the faulty conditions is on CTNOW configuration, too. Fig. 14 displays the signal voltages of healthy and faulty conditions.

$$R_{VTOW}(t) = 0.693\,e^{-4.04\times10^{-5}t} + 0.154\,e^{-6.23\times10^{-6}t} + 0.153\,e^{-6.43\times10^{-6}t} + 9.669e-07te^{-6.23\times10^{-6}t} + 1.215e-06te^{-6.43\times10^{-6}t} + 2.896e-12t^2e^{-6.23\times10^{-6}t} + 7.359e-18t^3e^{-6.23\times10^{-6}t} \quad (13)$$

$$R_{CTNOW}(t) = 0.662\,e^{-4.04\times10^{-5}t} + 0.149\,e^{-6.23\times10^{-6}t} + 0.189\,e^{-6.43\times10^{-6}t} + 1.136e-06te^{-6.23\times10^{-6}t} \quad (14)$$

$$R_{VTOW-DE}(t) = 0.154\,e^{-6.23\times10^{-6}t} - 0.154\,e^{-4.04\times10^{-5}t} + 9.669e-07te^{-6.23\times10^{-6}t} + 2.896e-12t^2e^{-6.23\times10^{-6}t} + 7.359e-18t^3e^{-6.23\times10^{-6}t} \quad (15)$$

$$R_{VTOW-SC}(t) = 0.153\,e^{-6.43\times10^{-6}t} - 0.153\,e^{-4.04\times10^{-5}t} + 1.215e-06te^{-6.43\times10^{-6}t} \quad (16)$$

$$R_{CTNOW-DE}(t) = 0.149e^{-6.23\times10^{-6}t} - 0.149\,e^{-4.04\times10^{-5}t} + 1.136e-06te^{-6.23\times10^{-6}t} \quad (17)$$

$$R_{CTNOW-SC}(t) = 0.189e^{-6.43\times10^{-6}t} - 0.189\,e^{-4.04\times10^{-5}t} \quad (18)$$

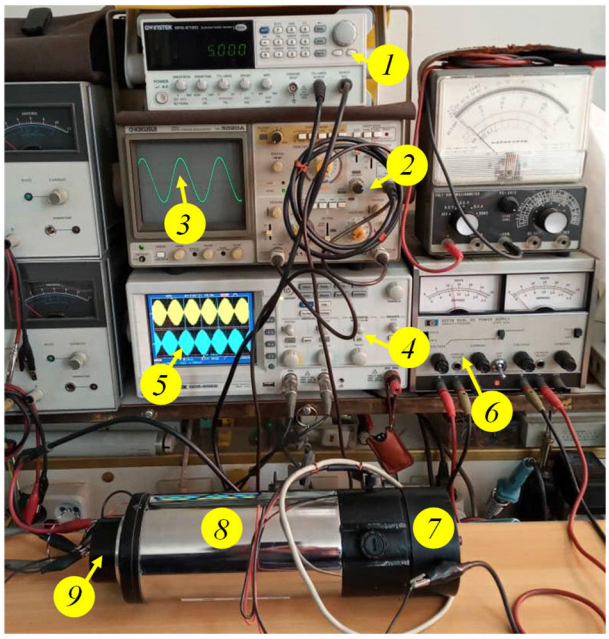

FIGURE 12. Experimental test setup, including (1) Function Generator, (2) Analog Oscilloscope, (3) Excitation Voltage, (4) Digital Oscilloscope, (5) Voltage Signals, (6) DC Power Supply, (7) Optical Encoder, (8) DC Motor, and (9) Built Resolver.

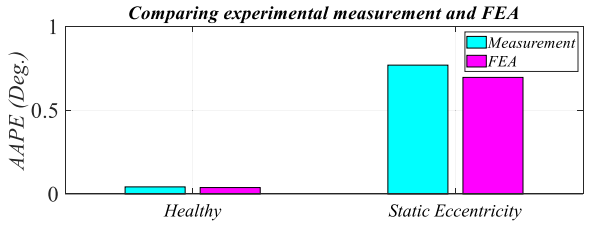

FIGURE 13. Verifying experimentally the FEA in healthy and faulty conditions (eccentricity 0.1 mm movement).

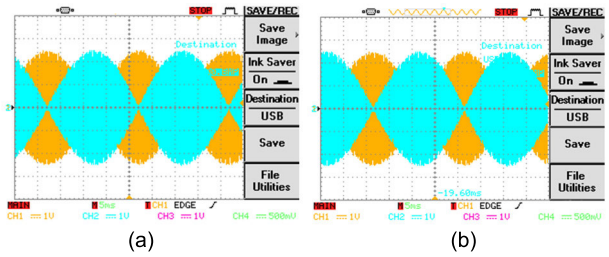

FIGURE 14. Comparing the signal voltages of the built resolver in both (a) healthy and (b) faulty conditions (0.1 mm static eccentricity).

V. CONCLUSION

This study suggested an effective reliability analysis for the resolvers, based on the Markov model, for the first time in the resolvers' field of study, according to the best of the author's knowledge. Our methodology has generality in applying to various resolvers' configurations. So, according to the WR resolver, the failure modes and failure rates were defined, respectively. By employing an experimentally verified resolver FE model, faulty conditions were injected into VTOW and CTNOW configurations of the VR resolver. Outcomes of FE analysis were as two states in the Markov model, steady or transient. Hence, VTOW and CTNOW configurations' reliability was investigated by analyzing the state's probability. Comparing VTOW and CTNOW shows the first one has more tolerability in signal winding SC and dynamic eccentricity. VTOW configuration has higher reliability according to MTTF, 19.77 years against 11.3 years in CTNOW configuration. Finally, to ensure the accuracy of the used FE resolver model, a prototype of investigated 1-X VR resolver with CTNOW configuration, which has higher error over VTOW configuration, was built and tested experimentally. Outcomes of the analysis can be a guide for choosing the resolver winding configuration optimally.

REFERENCES

[1] W. Li and M. Cheng, "Reliability analysis and evaluation for flux-switching permanent magnet machine," *IEEE Trans. Ind. Electron.*, vol. 66, no. 3, pp. 1760–1769, Mar. 2019, doi: 10.1109/TIE.2018.2838105.

[2] A. M. Bazzi, A. Dominguez-garcia, and P. T. Krein, "Markov reliability modeling for induction motor drives under field-oriented control," *IEEE Trans. Power Electron.*, vol. 27, no. 2, pp. 534–546, Feb. 2012, doi: 10.1109/TPEL.2011.2168543.

[3] H. Lasjerdi and Z. Nasiri-Gheidari, "A comprehensive analysis of short-circuit fault in wound-rotor resolvers," *IEEE Trans. Veh. Technol.*, vol. 69, no. 12, pp. 14884–14892, Dec. 2020, doi: 10.1109/TVT.2020.3043273.

[4] F. Totoonchian, "Effect of damper winding on accuracy of wound-rotor resolver under static-, dynamic-, and mixed-eccentricities," *IET Electr. Power Appl.*, vol. 12, no. 6, pp. 845–851, Jul. 2018, doi: 10.1049/iet-epa.2017.0777.

[5] M. KhajueeZadeh, H. Saneie, and Z. Nasiri-Gheidari, "Development of a hybrid reference model for performance evaluation of resolvers," *IEEE Trans. Instrum. Meas.*, vol. 70, pp. 1–8, 2021, doi: 10.1109/TIM.2021.3097409.

[6] X. Ge and Z. Q. Zhu, "A novel design of rotor contour for variable reluctance resolver by injecting auxiliary air-gap permeance harmonics," *IEEE Trans. Energy Convers.*, vol. 31, no. 1, pp. 345–353, Mar. 2016, doi: 10.1109/TEC.2015.2470546.

[7] Z. Nasiri-Gheidari, F. Tootoonchian, and F. Zare, "Design oriented technique for mitigating position error due to shaft run-out in sinusoidal-rotor variable reluctance resolvers," *IET Electr. Power Appl.*, vol. 11, no. 1, pp. 132–141, Jan. 2017, doi: 10.1049/iet-epa.2016.0316.

[8] K.-C. Kim, "Analysis on the charateristics of variable reluctance resolver considering uneven magnetic fields," *IEEE Trans. Magn.*, vol. 49, no. 7, pp. 3858–3861, Jul. 2013, doi: 10.1109/TMAG.2013.2246549.

[9] P. Naderi, R. Ghandehari, and M. Heidary, "A comprehensive analysis on the healthy and faulty two types VR-resolvers with eccentricity and inter-turn faults," *IEEE Trans. Energy Convers.*, vol. 36, no. 4, pp. 3502–3511, Dec. 2021, doi: 10.1109/TEC.2021.3079725.

[10] X. Shu, Y. Guo, W. Yang, K. Wei, Y. Zhu, and H. Zou, "A detailed reliability study of the motor system in pure electric vans by the approach of fault tree analysis," *IEEE Access*, vol. 8, pp. 5295–5307, 2020, doi: 10.1109/ACCESS.2019.2963197.

[11] S. A. M. Saleh, E. Ozkop, M. S. Ayas, T. Boileau, and B. Nahid-Mobarakeh, "Employing fault currents in the reliability analysis of motor drives," *IEEE Trans. Ind. Appl.*, vol. 56, no. 4, pp. 4521–4531, Jul. 2020, doi: 10.1109/TIA.2020.2975737.

[12] S. Samareh-TaheriNasab, M. KhajueeZadeh, Z. Nasiri-Gheidari, and S. Sheikhaei, "A low-cost linearized analog resolver-to-DC converter," in *Proc. 30th Int. Conf. Electr. Eng. (ICEE)*, May 2022, pp. 619–623, doi: 10.1109/ICEE55646.2022.9827090.

[13] M. KhajueeZadeh, M. Emadaleslami, and Z. Nasiri-Gheidari, "A high-accuracy two-stage deep learning-based resolver to digital converter," in *Proc. 13th Power Electron., Drive Syst., Technol. Conf. (PEDSTC)*, Feb. 2022, pp. 71–75, doi: 10.1109/PEDSTC53976.2022.9767427.

[14] R. Billinton and R. N. Allan, *Reliability Evaluation of Engineering Systems*. Boston, MA, USA: Springer, 1992, doi: 10.1007/978-1-4899-0685-4.

[15] H. Loge and L. Angerpointner, "The best way how to use resolvers," in *Proc. 1st Int. Electr. Drives Prod. Conf.*, Sep. 2011, pp. 208–213, doi: 10.1109/EDPC.2011.6085572.
[16] R. Ghandehari, P. Naderi, and L. Vandevelde, "Performance analysis of a new type PM-resolver in healthy and eccentric cases by an improved parametric MEC method," *IEEE Trans. Instrum. Meas.*, vol. 70, pp. 1–10, 2021, doi: 10.1109/TIM.2021.3080388.
[17] M. Bahari and F. Tootoonchian, "Proposal of a fault-tolerance technique for 1-ph open circuit fault in resolvers," *IEEE Sensors J.*, vol. 21, no. 14, pp. 15987–15992, Jul. 2021, doi: 10.1109/JSEN.2021.3076173.
[18] *Synchro and Resolver Engineering Handbook*, Moog Inc., Elma, NY, USA, 2013.
[19] J. G. Webster, *Measurement, Instrumentation, and Sensors Handbook*. Boca Raton, FL, USA: Chapman & Hall, 1999.
[20] M. Rausand and A. Hoyland, *System Reliability Theory: Models, Statistical Methods and Applications*, 2nd ed. Hoboken, NJ, USA: Wiley, 2005.
[21] *Military Handbook: Reliability Prediction of Electronic Equipment: MIL-HDBK-217F*, Department of Defense, Washington, DC, USA, 1991.
[22] *Quanterion Solutions Incorporated (U.S., Nonelectronic Parts Reliability Data 2016*, Qunanterion Solutions, Utica, NY, USA, 2015.
[23] *Carderock Division, Handbook of Reliability Prediction Procedures for Mechanical Equipment*, Carderock Division, Naval Surface Warfare Center, Bethesda, MD, USA, 1998.
[24] *FIDES Guide 2009 Edition A (English) | FIDES*. Accessed: May 3, 2022. [Online]. Available: https://www.fides-reliability.org/en/node/610
[25] P. Tattleman, "The MIL-STD-210C philosophy for establishing climatic requirements for military systems and equipment," in *Proc. 28th Aerosp. Sci. Meeting*. Washington, DC, USA: AIAA, 1990, p. 478.
[26] *Military Specification, Resolvers, Linear General Specification*, Standard MIL-R-50781, Oct. 25, 1972.
[27] *Military Specification, Resolvers, AC General Specification*, Standard MIL-R-23417B, Apr. 25, 1991.
[28] *Military Specification, Synchros, General Specification*, Standard MIL-S-20708E, Jun. 30, 1987.
[29] M. S. K. Zadeh, Z. Nasiri-Gheidari, and F. Tootoonchian, "Study of noise and vibration in wound rotor resolvers," in *Proc. 28th Iranian Conf. Electr. Eng. (ICEE)*, Aug. 2020, pp. 1–5, doi: 10.1109/ICEE50131.2020.9260668.
[30] M. S. KhajueeZadeh, S. Feizhoseini, Z. Nasiri-Gheidari, and M. Behzad, "Analysis of torsional vibrations on the resolver under eccentricity in PMSM drive system," *IEEE Sensors J.*, vol. 22, no. 22, pp. 21592–21599, Nov. 2022, doi: 10.1109/JSEN.2022.3209991.

MAHDI EMADALESLAMI (Student Member, IEEE) received the B.Sc. degree in electrical engineering from the Shahid Bahonar University of Kerman (SBUK), Kerman, Iran, in 2018, and the M.Sc. degree in power system from the Tarbiat Modares University, Tehran, Iran, in 2021. His current research interests include power system reliability analysis and application of artificial intelligence and data science in power systems.

MOHAMMADSADEGH KHAJUEEZADEH was born in Kerman, Iran, in 1996. He received the B.Sc. degree (Hons.) in electrical engineering from the Faculty of Electrical Engineering, Shahid Bahonar University of Kerman (SBUK), Kerman, in 2018, and the M.Sc. degree (Hons.) in electrical engineering from the Department of Electrical Engineering, Sharif University of Technology (SUT), Tehran, Iran, in 2021. His current research interests include performing finite element analysis (FEA), reliability analysis, vibration analysis, and artificial intelligence (AI)-based fault diagnosis of electrical machines and electromagnetic sensors.

MOHAMMADEBRAHIM ZAREI received the B.Sc. degree in electrical engineering from the Shahid Bahonar University of Kerman (SBUK), Kerman, Iran, in 2018, and the M.Sc. degree in power system from the Tarbiat Modares University, Tehran, Iran, in 2022. His current research interests include power system reliability analysis and smart grids.

MAHMOUDREZA HAGHIFAM (Senior Member, IEEE) received the B.Sc. degree in electrical engineering from the University of Tabriz, Tabriz, Iran, in 1988, the M.Sc. degree in electric power system engineering from the University of Tehran, Tehran, Iran, in 1990, and the Ph.D. degree from Tarbiat Modares University, Tehran, in 1995. In 1995, he joined the Faculty of Electrical and Computer Engineering, Tarbiat Modares University, where he is currently a Professor. He is the author of four book chapters published by Springer and seven text books. His research interests include power system reliability analysis, smart electric distribution networks, and data analysis in power system operation. He was a recipient of research scholarships from DAAD and AvH in Germany several times for research stay in Aachen Technical University (RWTH), Aachen, Germany. He is a member of Directing Committee of CIRED. He acted as the Vice Chairperson for electric distribution and a member of the Directory of Tavanir, Tehran, for four years. He is currently the Vice President for Research and Technology with MAPNA Group, Tehran.

HADI TARZAMNI (Student Member, IEEE) was born in Tabriz, Iran, in 1992. He received the B.Sc. and M.Sc. degrees (Hons.) in power electrical engineering from the Faculty of Electrical and Computer Engineering, University of Tabriz, Tabriz, in 2014 and 2016, respectively. He is currently pursuing the dual Ph.D. degree in power electronics engineering with the Department of Electrical Engineering, Sharif University of Technology, Tehran, Iran, and the Department of Electrical Engineering and Automation, Aalto University, Finland. He has authored and coauthored more than 30 journal and conference papers. He also holds six patents in the area of power electronics. He was a recipient of Best Paper Award in 10th International Power Electronics, Drive Systems and Technologies Conference (PEDSTC), in 2019. He has been awarded a three-year Aalto ELEC Doctoral School Grant, and a Jenny and Antti Wihuri Foundation Grant, in 2021 and 2022, respectively. Since January 2021, he has been a Researcher with the Department of Electrical Engineering and Automation; and the Department of Electronics and Nanoengineering, Aalto University, Finland. His research interests include power electronic converters analysis and design, DC–DC and DC–AC converters, high step-up power conversion, soft-switching and resonant converters, and reliability analysis.